Proceedings of BS2013:
13th Conference of International Building Performance Simulation Association, Chambéry, France, August 26-28

DESIGN OPTIMIZATION OF DAYLIGHT ROOFING SYSTEMS: ROOF MONITORS WITH GLAZING FACING IN TWO OPPOSITE DIRECTIONS

Ladan Ghobad, Wayne Place, and Soolyeon Cho
North Carolina State University

ABSTRACT

This research focuses on design optimization of roof daylighting systems in office buildings. The optimization is based on computer simulation of daylighting and overall energy performance. This research builds on previous work published by the authors that discussed design issues for skylights to increase the potential electric light saving through the use of daylight. This study extends the previous work to investigate roof monitors with vertical apertures facing in two opposite directions (north-south). The purpose is to evaluate daylighting performance of roof monitors and account for the associated thermal impacts, specifically the effect of solar radiation gains on heating and cooling loads of the building. This paper attempts to provide design suggestions for roof monitors, provide optimization information for aperture sizing and spacing, and report savings in energy consumption and operation costs in two distinct climates.

INTRODUCTION

Although daylight can be admitted through any aperture in building, achieving the most efficient and effective interior illumination with sunlight requires care in the placement and design of the illumination glazing. Improper design creates visual discomfort, excessive solar heat gains and higher cooling and heating loads in buildings.

Roof monitor is one of the rooflight configurations defined by CIBSE nomenclature (Baker and Steemers, 2002). The monitor rooflight has vertical glazing in two opposite directions. In this study, north and south orientation is preferred because the south-facing glazing can easily be shaded and the north-facing glazing only admits diffuse daylight to the space.

Some case studies of roof monitors were illustrated by Fontoynont (1999). Assessment of the potential for energy saving in commercial buildings with roof monitors has been previously investigated (Place et al., 1984, Fontoynont et al., 1984). However, those studies lack construction details that inform how the building is assembled and some crucial factors, such as the depth of light-wells, were ignored in simulations.

Furthermore, this study uses Radiance (Ward, 1994) and DAYSIM (Reinhart and Walkenhorst, 2001), which are validated and proved to be more accurate than the built-in algorithms used in whole-building energy simulation tools such as DOE-2 for lighting simulation (An and Mason, 2010, Guglielmetti and Scheib, 2012).

The main questions to be addressed in this paper are: How should roof monitors be configured to optimize the trade off between reducing lighting electricity consumption and keeping cooling energy costs under control? How much operating energy and operating cost can be saved with such an optimized roof monitor system?

BUILDING PARAMETERS

The baseline parameters for the building in this paper are:

1. An office space of dimension 30-ft x 30-ft (9.14m x 9.14m) was modeled to represent a section cut from an infinite rooflit space. To avoid complicating the outputs with wall or partition effects, this space has been surrounded on all sides by eight other identical spaces in the daylighting model. Readers should remain cognizant of the fact that introducing partitions or walls will complicate the analysis and substantially alter the results.
2. The insulated, opaque portions of the roof consist of 7-in. (0.18 m) thick Styrofoam with U-value of 0.187 W/m^2K to be in compliance with ASHRAE Standard 90.1-2010 and regional building codes in the United States.
3. The single roof monitor, located at the middle of space, extends along the length of the module creating linear, vertical apertures facing north and south (figure 1).

Table 1

Glazing dimensions in roof monitors with various AFRs

AFR	WIDTH AND LENGTH OF MODULE	REDUCTION FACTOR ON THE HORIZONTAL GLAZING DIMENSION (accounting for diagonal and vertical truss webs)	EFFECTIVE HORIZONTAL DIMENSION OF THE GLAZING	GLASS AREA IN ONE PANEL	HEIGHT OF THE GLASS
	m		m	m^2	m
0.15	9.14	0.9	8.2	6.27	0.76
0.20	9.14	0.9	8.2	8.28	1.01
0.25	9.14	0.9	8.2	10.53	1.28

4. The roof decking is supported by trusses in the vertical apertures and extending down into the opaque light well.
5. The height of roof, from finished floor to top of the curb under the glazing, is 13'-7" (4.14 m) in all cases. Therefore, the distance between the lower edge of the glazing to task-level remains constant in all cases.
6. The high portion of the roof (top of the monitor) is horizontal.
7. The low portion of the roof (between the monitors) slopes at 0.25 in. of fall per foot of horizontal run (2 cm fall per meter). Over 30 feet of horizontal run, this will be a drop of 7.5" (0.19m). For 60 feet of horizontal run, this will be a drop of 15.0 in (0.38m). This slope is accommodated by a variable height curb beneath the glass.
8. The curb height at the high end is 4" (0.10m) and at the low end is 11.5" (0.29m). Curbs are 3.5" (0.09m) thick, composed of 1.5" (0.04m) wood and 2" (0.05m) styrofoam for insulation purposes. The overall U-value of the curb is 0.6 [W/m^2-K].
9. The sloping portion of the roof accommodates water runoff and provides a tapered plenum volume beneath it to conduct air for thermal conditioning and fresh air.
10. Longer runs of the roofing system will require deeper structure and a deeper plenum volume to conduct the required air for thermally conditioning the larger space. The deeper structure and plenum volume will require a deeper light well. For the purposes of this paper, two light-well depths were examined: 24 in. deep (0.61m) and 36 in. deep (0.91m)
11. All vertical and horizontal dimensions are shown in Tables 1 and Figure 1.
12. This roofing configuration can accommodate some private offices, but it generally lends itself better to open office arrangements, which is what was assumed in this study.
13. The south-facing aperture is double glazing composed of Velux Laminated glass with Low-e coating and a layer of clear glass with Argon gas in the middle. This composite of layers result in a diffuse glazing material with visible transmittance of 57%, which is appropriate to equalize beam sunlight.
14. On north-facing aperture is a double glazing consisting of two layes of clear glass resulting in visible transmittance (Vt) of 72%.
15. The actual visible light transmittance through the glazing is reduced by approximately 10% by the obstructing effect of the truss web members. As a result, the actual Vt of south facing and north facing apertures would be 51% and 65% respectively.
16. The SHGC is 0.386 for south-facing and 0.312 for north-facing glass. Properties of glazing materials were acquired from the Lawrence

Table 2

U-values of vertical aperture assemblies

AFR	AREA OF GLAZING	U AVERAGE OF GLAZING	GLAZING UA	AREA OF CURBS	U AVERAGE OF CURB	CURB UA	OVERALL UA	ASSEMBLY AVERAGE U-VALUE
%	m^2	W/m^2K	W/K	m^2	W/m^2K	W/K	W/K	W/m^2K
15	6.27	1.86	11.65	2.25	0.60	1.35	13.00	2.07
20	8.28	1.78	14.70	2.25	0.60	1.35	16.05	1.94
25	10.53	1.73	18.20	2.25	0.60	1.35	19.55	1.86

Berkeley National Laboratory WINDOW 6.3 simulation tool.

17. The U-value of the center of the glass is 1.42 [W/m^2-K] for both north and south facing glass.
18. The total U-value of the glazing assembly is calculated based on an area-weighted average of the components (table 2), which are: glazing and curbs. Average U-value of glazing itself is estimated by accounting for the effect of edges and frames for each panel of glass with 7.5' (2.29m) length. Table 4 shows the results.
19. Overhangs for the south facing glazing is designed to avoid some of the direct beam light. The projection of the south ovehang is proportional to the glass height, thereby prodducing a 12° angle of rejection between the surface of the glazing and the end point of the overhang. The north glazing has a minimal overhang of 2" (0.05m) projection, to accommodate detailing.

The parametric variations in the study are:

1. Building locations: Boston and Miami. These two locations were selected because they represent two substantially different climates in terms of daylight availability and thermal conditions in the United States.
2. The depth of the light-well through which the daylighting is entering:
   - 24 in. (0.61m) deep light well, with a floor to ceiling dimension of 11' 6 ¾" (3.52m).
   - 36 in. (0.91) deep light well, with a floor to ceiling dimension of 10' 6 ¾" (3.22m).
3. The glazing area, expressed as the **A**perture-to-**F**loor-Area **R**atio (AFR):
   - 15%, 20% and 25%

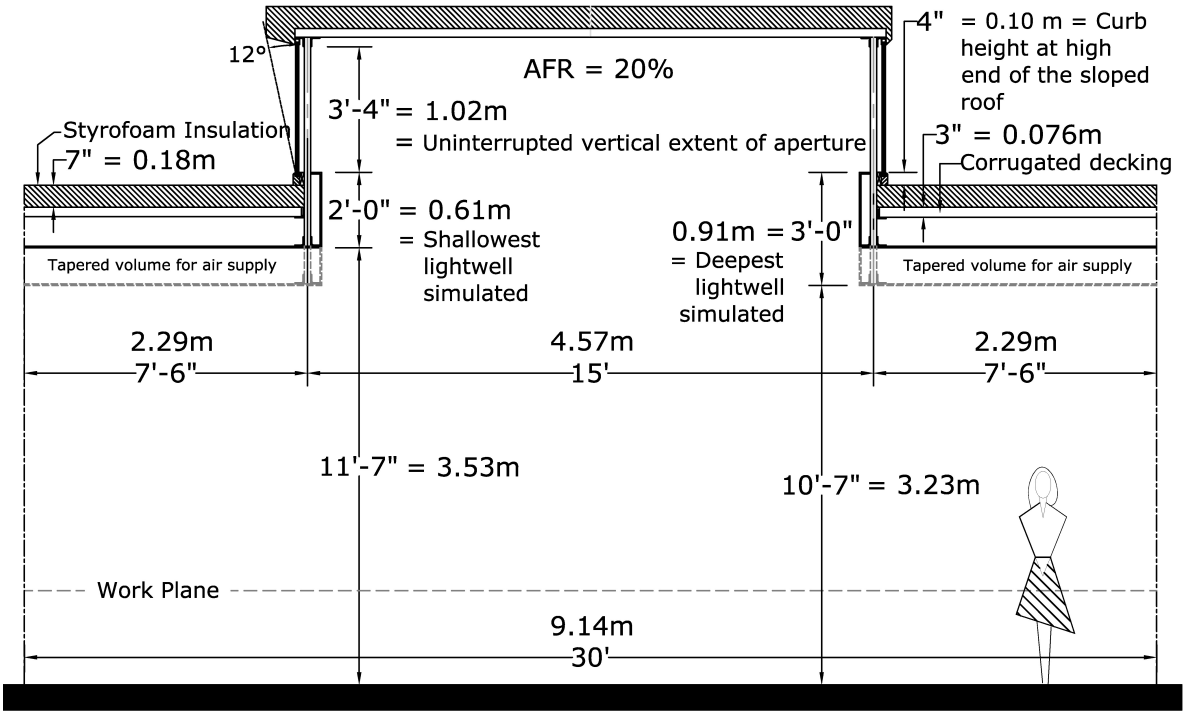

Figure 1 Roof monitor section

SIMULATION

The analysis is performed in several stages. The roof daylighting models were drawn in Rhinoceros. DIVA-for-Rhino was used for daylighting and whole-building simulation. DIVA 2.0 is a plug-in to Rhino that exports scene geometries, material properties, and sensor grids into the format required to enable the use of Radiance, DAYSIM and EnergyPlus (Lagios et al. 2010).

In simulation process: (1) Illuminance distribution across the task surface was computed for a single moment in time using Radiance. (2) Annual interior illumination was assessed using DAYSIM. (3) Whole-building energy simulation was performed with EnergyPlus. (4) Operating energy was computed for the different categories of use in the building. (5) Total energy operating costs (in dollars) were calculated for each daylighting system to make comparisons and suggest design optimizations.

Annual interior illumination was assessed by DAYSIM. Electric lighting schedules, generated in format of Excel CSV files from DAYSIM, were the most important inputs to EnergyPlus to assess electric light savings due to the use of natural light. For single-time simulations, Radiance parameters: ambient bounces (ab) 8, ambient division (ad) 3600, ambient super-samples (as) 900, ambient resolution (ar) 600, ambient accuracy (aa) 0.05 were selected. These parameters were adjusted until smooth curves were achieved and illuminance values converged to consistent results. For annual simulations lower parameters were selected due to much longer time requirement: ab 7, ad 2500, as 625, ar 300, aa 0.05.

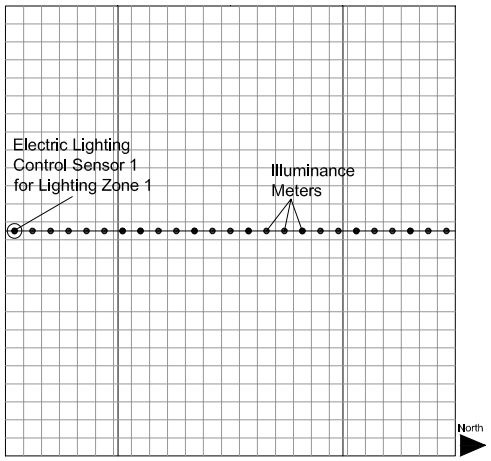

Figure 2 Floor plan with locations of illuminance meters and photosensor

The illuminance target in models was 300 lux, which provides suitable lighting condition for computer-based office work (IES). Illuminance levels were collected in a 25x25 grid at task level 2.5' (0.76m) above the finished floor in Radiance simulation program. A single sensor controlled the electric lighting. The sensor was located at the boundary of the space where the least illuminance occurred in the module (figure 2). Future research will address more electric lighting zones with additional sensors to control the electric lights more finely to the needs of the various parts of the space.

Electric lighting was a continuous dimming control system that controled 100% of lighting fixtures in the models. Figure 3 shows the electric power input to lighting fixtures as a function of daylight illuminance at the photosensor's location. Based on the electric lighting power input and electric lighting density, EnergyPlus calculated electric lighting consumption for the interior spaces.

In simulations, the standby power was assumed to be zero rather than the typical 20%-30% power drawn for dimming control for fluorescent luminaires (figure 3). This assumption was made regarding emerging improvements in the field of LED lighting, which draws much lower electric power when enough daylight is available. Studies already in the works by the authors will address fluorescent fixtures, with the appropriate standby power for that technology.

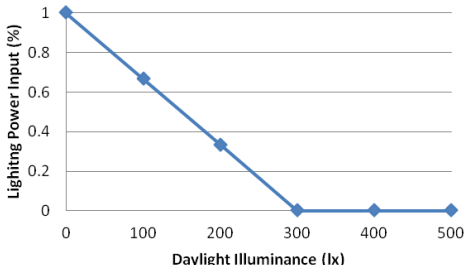

Figure 3 Power input curve of the continuous dimming lighitng control used for DAYSIM schedules

The thermal models were generated along with the daylight models in Rhino, with the same dimensions but less architectural details and in a separate layer. DIVA generates the idf file, which contains geometric information of the models. The idf file is modified in EnergyPlus 7.0.0.036 and further parameters such as construction materials, internal loads, operation schedules, and HVAC system were inserted.

All the 30' (9.14 m) x 30' (9.14 m) modules were simulated as single thermal zones with four adiabatic walls and an adiabatic ground, representing an interior space of a large well-insulated rooflit office building. The installed lighting power density for the building was modelled as 9.68 Watt/m^2 based on ASHRAE 90.1-2010 for commercial buildings. Office equipment for each module was composed of four computers, a printer, a scanner and a copier, resulting in 886 watts heat generation. Four people occupied each thermal zone during weekdays from 9 am until 5 pm and required total of 0.0378 (cubic meter per second) ventilation (ASHRAE 90.1-2010). No air infiltration existed in the models because of having four adiabatic walls.

The HVAC system was composed of the following components: outdoor air mixing box, AC unit (cooling coil), gas furnace, humidifier, fan, air splitter, air terminal with reheat, and mixing box. The cooling system employed a direct-expansion DX cooling coil with single speed. The AC system used electricity with COP (Coefficient of Performance) of 3. The heating system was a natural gas furnace with COP of 0.8.

Simulations were conducted with heating setpoint 22°C from 4am to 7pm and heating setback 17°C. Cooling setpoint was 24.5°C from 5am to 8pm and cooling setback was 32°C. The thermostat performed based on operative temperature because it is a more accurate indicator for thermal comfort rather than mean air temperature (ASHRAE 55-2010). For the

purposes of this study, operative temperature was defined as:

$$T_{opt} = 0.55\ _{MRT} + 0.45\ _{Mean\ Air\ Temp} \quad (1)$$

which corresponds to a still air situation. For situations with somewhat more air movement, a weighting of 50-50 between MRT and mean air temperature is commonly used.

RESULTS AND DISCUSSION

Daylighting

Figure 4 shows single-time illuminance simulations for 20% AFR monitors in Boston and Miami for a sunny, equinox day. Two light-well depths were simulated for Boston: squared-off light-wells with 0.61 m vertical dimension and squared-off light-wells with 0.91 m vertical dimension. The roof monitor with deeper wells has 1.02 times the average illuminance of the other one. In other words, the effect of depth of the light well on illumination performance is very small for this range of variation in light-well depth.

The simulations indicate that the average illuminance in the middle axis of the space in Miami is about 85% of the average illuminance of the same space in Boston. This is due to higher incidence of solar radiation on vertical surfaces when the altitude angles are lower; the altitude angle at equinox noon is 47° in Boston and 65° in Miami.

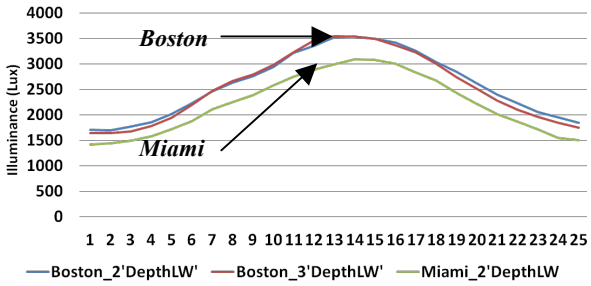

Figure 4 Illuminance distribution [lux] in single roof monitors with 20% AFR in Boston and Miami

A major purpose of this study was to find the optimum aperture area for roof monitors in terms of minimizing annual energy operating costs. At small aperture areas, lighting electricity reduction is expected to be the dominant energy impact of introducing the apertures. At larger aperture areas, the lighting electricity saving begin to taper off and are eventually overcome by the thermal impacts of conductive losses during the heating season and excess solar gains during the cooling season. To facilitate identifying the optimal glazing area, multiple apertures sizes were studied: 15%, 20%, and 25% AFR (**A**perture-to-**F**loor-area **R**atio). AFRs less than 15% were regarded as impractical for both construction and aesthetic reasons. Illuminance distributions at equinox noon are plotted for AFR variations of monitors at the middle north-south axis at task level for Boston and Miami (figure 5). Table 3 summarized the average illuminance levels in all cases.

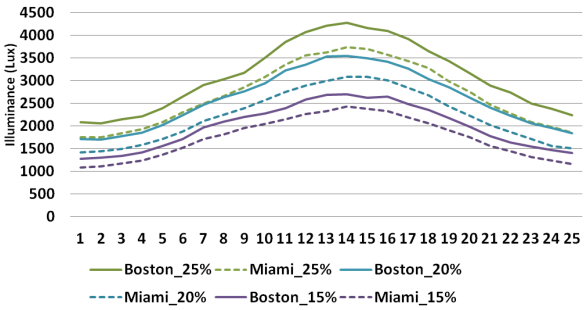

Figure 5 Illuminance distributions [lux] for various AFRs in Boston and Miami

Table 3 Average daylight illuminance

	AVERAGE ILLUMINANCE (LUX)		
AFR	15%	20%	25%
Boston	1981	2593	3106
Miami	1737	2217	2693

Electric lighting

Figure 6 shows daily average lighting electricity use of single roof monitors in Boston and Miami, as it varies by month. The base case, which is modelled with an opaque roof, has 6.49 [kWh] average daily use of lighting electricity. In figure 6, the base case lighting electricity consumption has not been plotted because it would drastically stretch out the graph and make it difficult to see other variations of interest. The lighting electricity consumption goes below 1.0 kWh usage for ever roof monitor configuration. This rapid decrease primarily reflects the influence of beam sunlight, which is intense enough to displace substantial amounts of the electric light.

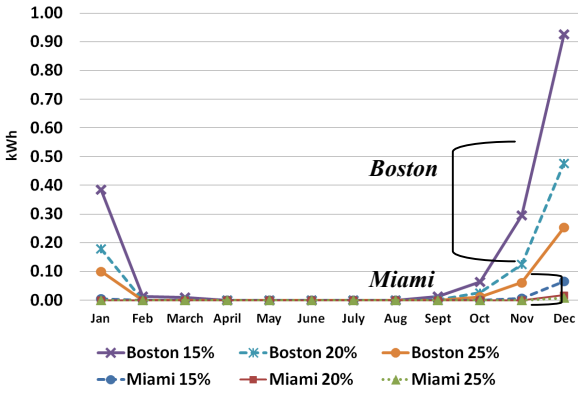

Figure 6 Daily average electric lighting Use (by month) [kWh] Boston and Miami

Although Boston had higher average illumination at equinox noon than Miami (figure 4 and 5), electric lighting use in Boston is higher in wintertime due to fewer hours of daylight and higher cloud cover. As a result, roof monitors perform better in Miami in the heating season in terms of daylighting performance.

Figure 6 shows that with roof monitors, enough daylight is available for most of the months. Vertical monitors that face south and north cause effective collection for most hours of a day. Furthermore, vertical glazing collects effectively during summer and even during winter when solar altitude angles are lower. The largest difference between variations of AFR occurs in November, December, and January. Particularly, Boston requires more electric lighting than Miami in these months due to lower sun angles and fewer sunshine hours that reduce available outside illumination.

The curves in figure 6 are drawn based on occupancy schedule from 9am until 5pm on weekdays. Longer hours of building operation will increase the electric load because there is little or no daylight available in early and late hours of a day.

Heating and cooling energy consumption

Heating fuel consumption and cooling coil electric consumption (by month) [kWh] are shown for single monitors with different AFRs in Boston and Miami in figures 7 and 8. The base case is shown to compare spaces with vertical apertures to the same space with no apertures on the roof. Single roof monitors are designed with 0.61m light-wells. The purpose was to select the optimum **A**perture-to-**F**loor-Area **R**atio (AFR) which admits substantial sunlight and solar radiation during the heating season and which satisfies most of the summertime illumination needs without overloading the building.

In figure 7, the monthly energy consumption of the gas furnace is plotted for various roof aperture areas, for roof monitors. With adding roof monitors, heating fuel consumption increases significantly from the base case, because of increased conductive losses associated with adding glazing to the roof and the replacement of electric light with sunlight of lower heat content. As the area of apertures increases from 15% to 25%, heating fuel consumption increases at a lower rate. The reason is that solar gains compensate the combined effect of reduced heat from the electric lights and increased conductive losses associated with increased glazing area.

In Miami, there is heating coil energy use in both heating and cooling seasons. The reason for having gas use for furnace even in cooling season is that the HVAC loop requires heating for dehumidification process in Miami. In Miami, cooling coil consumption (figure 8) is more sensitive than heating fuel consumption (figure 7) to variations in the aperture area. This is because of higher cooling degree days in Miami and higher requirement for cooling when excessive solar heat gain is received through the glazing. In both cities, as the area of vertical glazing increases, the cooling coil electric use increases.

Energy use intensity

In figures 9 and 10, energy use per unit of floor area per year EUI [kWh/m^2/yr] is categorized by type of energy consumption: equipment, fan, lighting, cooling, heating and humidifier in order to understand the contribution of each category separately.

Results show the most potential saving by the use of horizontal apertures occured for electric lighting enery consumption in both Boston and Miami. Furthermore, results show that in both Boston and Miami, the lowest energy use for spaces with roof monitors occurs at the lowest aperture area somewhere around 15% AFR. In addition, vertical roof apertures create higher potentials for whole-building enrgy saving in Miami than Boston do due to better daylighting performance and lower heat loss through glazing in Miami.

In figure 9, results from Boston show that adding vertical apertures to the base case increases the annual energy use per square unit of area. The reason is that heat loss through the apertures is so high that the benefits of solar heat gain through the glazing becomes negligible. Increasing the size of aperture requires higher heating gas consumption to compensate for more heat loss. Large heating energy requirement in Boston is associated with high heating degree-days created as a result of large hourly temperature differences between inside and outside during the heating season.

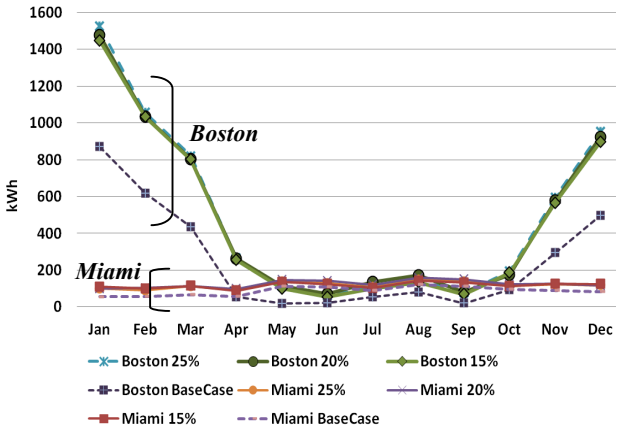

Figure 7 Monthly heating coil gas consumption [kWh]

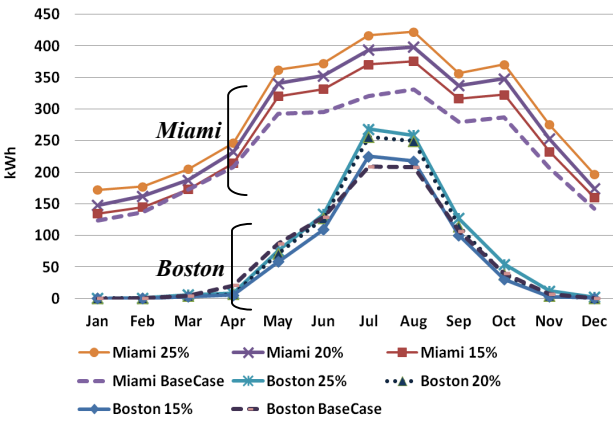

Figure 8 Monthly cooling coil electricity [kWh]

However, in Miami (figure 10), the energy consumption falls sharply with increasing glazing area, because of the decrease in lighting electricity. At smaller apertures, energy use for heating and cooling slightly increased in Miami, however, the benefit of electric lighting reduction is more significant, which creates a net reduction in whole-building energy use. At 25% AFR, when roof monitors have almost no energy savings from the base case; as the aperture area increases (larger than 25%) excessive solar heat gain negates the benefits of daylighting.

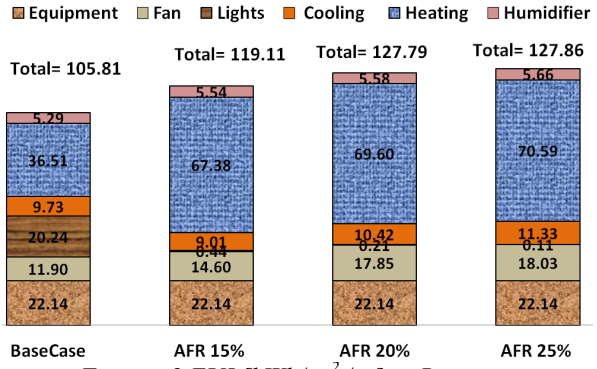

Figures 9 EUI [kWh/m ^{2}/yr] in Boston

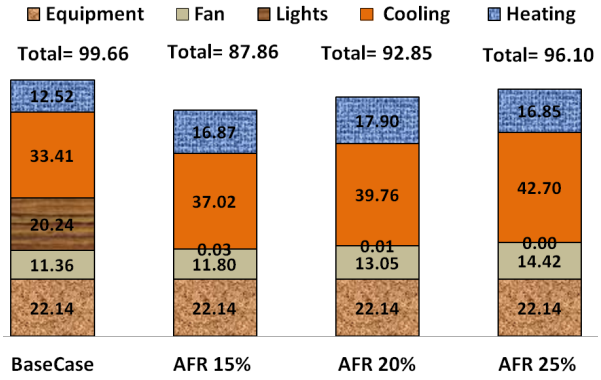

Figures 10 EUI [kWh/m ^{2}/yr] in Miami

BUILDING OPERATION COSTS

Figure 11 shows the annual operating cost for energy as a function of AFR in modules with 900 ft^2 (83.6 m^2) floor area with single monitors in Boston and Miami. The operation costs were calculated based on the local cost for electricity and gas, which were both higher in Boston than Miami. Contribution of electric and gas consumption to the total cost is reflected in figure 11. The cost per unit of energy at both sites was higher for electricity than it was for gas. As a result, the variations in electricity as a function of AFR were more significant from an energy economics point of view. Figure 11 also depicts the total savings associated with the area of apertures

In Boston, for commercial buildings, the price of electricity was \$0.0548 per kWh in Oct-May and \$0.0828 per kWh in June-Sep plus a monthly fee (NSTAR). Gas price in Boston was \$0.0196 per kWh. In Miami, electricity costs \$0.0469 per kWh and gas price for commercial buildings, which use 0-2000 annual therms, was \$0.0116 per kWh plus a monthly fee (FLP).

In both locations, costs decrease rapidly with the introduction of the vertical apertures at 15% AFR due to reductions in lighting electricity consumption (see figures 9 and 10). Beyond an optimum aperture area, increases in heating fuel consumption in Boston and rises in cooling electricity in Miami exceed the decreases in lighting electricity. As a result, the costs increase with increasing aperture area.

Figure 11 compares vertical apertures in terms of operating cost for energy in modules with different AFRs in Boston and Miami. Benefits of roof monitors are higher in warmer climates such as Miami with less heating degree-days. As expected, the Miami curves reach the minimum operation cost, which reflects the generally warm and sunny character of Miami and also lower operation costs in this city compared to Boston.

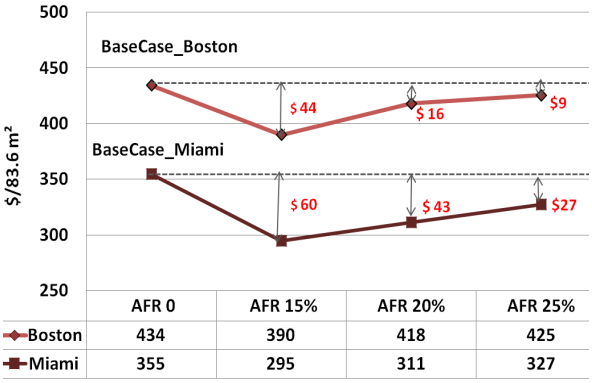

Figure 11 Building operation costs [\$ per module of 83.6 m^2] in Boston and Miami

The most potential cost benefits are achieved at 15% AFR for single roof monitors at both climates. Roof monitors with optimum aperture area can save \$0.05 per ft^2 (\$0.53 per m^2) of floor area per year in Boston and \$0.07 per ft^2 (\$0.72 per m^2) of floor area per year in Miami. Results show that an economically optimum roof monitor saves 98%-100% of annual lighting energy consumption in Boston and Miami respectively.

CONCLUSIONS

Energy performance analysis of vertical apertures requires accurate monitoring of thermal impacts as well as lighting impacts of roof monitors. Larger aperture areas are appreciated in terms of lighting but depreciated in terms of heating and cooling. The optimum design for roof monitors facing north and south occur at apertures with 15% AFR as figure 11 illustrated.

Vertical apertures facing south have the benefit of receiving winter sun and rejecting summer sun that balance some of the heating and cooling loads. But in cold climates such as Boston, large heat loss through the glazing assembly degrades thermal benefits of roof monitors. For cold climates, more stringent U-values are required to increase performance of roof monitors. However, using a triple glazed window with highly insulated frame will increase the cost of roof monitors.

In interpreting these results, it is useful to revisit some of the assumptions in the simulation:

1. These studies were performed for a target illuminance of 300 lux on the work plane, which is at the very low end of what we would prescribe in office spaces; 550 lux would be more common. The expected energy benefits of the roof monitors would be substantially increased for a higher target illuminance. In a sense, this study is the worst-case scenario for assessing the potential of using daylighting from roof monitors for interior illumination in that we have accepted a very low illuminance level for the expressed purpose of reducing energy consumption through conservation. "Free" daylighting gives us the option to seek a light level that would be much more optimal from a human point of view.
2. A furnace of 80% efficiency was assumed in this study. Improving furnace efficiency would reduce the negative cost impacts of heat loss through the roof monitors.
3. Alternate glazings with lower U-values would make the system thermally more effective.
4. In the final analysis, the greatest motive for introducing daylighting into a building is the life-quality issue. In the light of that fact, we should not imagine that we had done proper "economic analysis" when we have only consider the benefit of reduced energy operating cost.

Studies are already in the works to explore a much wider range of these parameters.

ACKNOWLEDGEMENT

This paper is result of the research conducted for Ph.D. dissertation of the first author during Fall 2012 at North Carolina State University. Professor Place was the chair and Professor Cho was on the committee. Thanks to Christoph Reinhart and Alstan Jakubiec, who were truly helpful with the queries related to DIVA.

REFERENCES

American Society of Heating Refrigerating and Air-conditioning Engineers (ASHRAE) Standard 90.1-2010 and Standard 55-2010.

An, J., and Mason, S. 2010. Integrating Advanced Daylight Analysis into Building Energy Analysis. Proc. Fourth National Conference of IBPSA-USA, New York, NY.

Baker, N., and Steemers, K. 2002. Daylight design of buildings. London: James & James.

Fontoynont, M., Place, W., and Bauman. F. 1984 Impact of Electric Lighting Efficiency on the Energy Saving Potential of daylighting from roof monitors. Energy and Buildings 6.4 (1984): 375-386.

Fontoyont, M. 1999. Daylight performance of building. Routledge.

Illuminating Engineering Society (IES). Lighting Level Recommendations.

Ghobad, L., Place, W., & Hu, J. 2012. The impact of systems integration on the daylighting performance of skylights in offices. Conference Proceeding of SimBuild 2012, Madison, USA.

Guglielmetti, Rob, and Jennifer Scheib. 2012. Challenges to integrated daylighting and electric lighting simulation methods in a whole-building energy simulation context. Conference Proceeding of SimBuild 2012, Madison, USA.

Lagios, K., Niemasz, J., & Reinhart, C. F. 2010. Animated Building Performance Simulation (Abps) – Linking Rhinoceros/ Grasshopper With Radiance/ Daysim. Conference Proceedings of SimBuild 2010, New York City, USA.

Larson, G. W. 1998. Rendering with radiance : The art and science of lighting visualization.

Place, W., Fontoynont, M., Conner, C., Kammerud, R., Andersson, B., Bauman, F., Carroll, W. L., Howard T.C., Mertol. A. & Websster. T. 1984. Energy and Buildings, 6 (1984) 361-373.

Place, W., Coutier, P., Fontoynont, M., Kammerud, R., Andersson, B., Bauman, F., Carroll, W. L., Wahlig, M., & Thomas L. W. 1987. The Impact of Glazing Orientation, Tilt, and Area on the Energy Performance of Roof Apertures, ASHRAE Transactions, Vol. 93, Part 1A, New York, January 1987.

Reinhart, C.F. and Walkenhorst, O., 2001. Validation of dynamic RADIANCE-based daylight simulations for a test office with external blinds. Energy and Buildings, 33, 683–697.

Ward, G. 1994. The RADIANCE lighting simulation and rendering system. In: Proceedings of the 21st annual conference on computer graphics and interactive techniques. SIGGRAPH. New York: ACM, 459–472.